Ecotoxicology and Environmental Safety 264 (2023) 115400

Contents lists available at ScienceDirect

Ecotoxicology and Environmental Safety

journal homepage: www.elsevier.com/locate/ecoenv

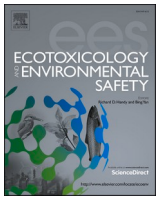

Desorption of sulfamethoxazole from polyamide 6 microplastics: Environmental factors, simulated gastrointestinal fluids, and desorption mechanisms

Kefu Wang [a], Kangkang Wang [a], Yaoyao Chen [a], Siqi Liang [a], Yi Zhang [b], Changyan Guo [a,*], Wei Wang [c,*], Jide Wang [a,*]

[a] Key Laboratory of Oil and Gas Fine Chemicals, Ministry of Education & Xinjiang Uygur Autonomous Region, School of chemical engineering and technology, Xinjiang University, Urumqi, China
[b] College of Chemistry and Chemical Engineering, Central South University, Changsha 410083, China
[c] Department of Chemistry and Center for Pharmacy, University of Bergen, Bergen N-5007, Norway

ARTICLE INFO

Editor: Richard Handy

Keywords:
Polyamide 6 microplastic
Sulfonamide antibiotics
Sorption behavior
Gastrointestinal conditions
Desorption mechanisms

ABSTRACT

Microplastics (MPs) can enrich pollutants after being released into the environment, and the contaminants-loaded MPs are usually ingested by organisms, resulting in a potential dual biotoxic effect. In this paper, the adsorption behavior of Sulfamethoxazole (SMX) on Polyamide 6 (PA6) MPs was systematically investigated and simulated by the kinetic and isotherm models. The effect of environmental conditions (pH, salinity) on the adsorption process was studied, and the desorption behavior of SMX-loaded PA6 MPs was focused on simulating the seawater, ultrapure water, gastric and intestinal fluids. We found that lower pH and solubilization of SMX by gastrointestinal components (bovine serum albumin (BSA), sodium taurocholate (NaT), and pepsin) can reduce the electrostatic interaction between the surface charge of PA6 MPs and SMX. The result will lead to an increase in the desorption capacity of SMX-loaded PA6 MPs in gastrointestinal fluids and therefore will provide a reasonable mechanism for the desorption of SMX-loaded PA6 MPs in the gastrointestinal fluids. This study will provide a theoretical reference for studying the desorption behavior of SMX-loaded PA6 MPs under gastrointestinal conditions.

1. Introduction

When plastic wastes are inevitably introduced into the environment, longtime exposure usually leads to changes in their mechanical and physicochemical properties (Thompson et al., 2004). The changes in properties can result in the formation of plastic fragments, which are called microplastics (MPs) when they are < 5 mm in size (Cole et al., 2011). In recent years, MPs pollution has been found in a variety of environments around the world, and it is considered to be a potential threat to the ecosystem and human health (Bradney et al., 2019; Stollberg et al., 2021). In an aqueous environment, low-density MPs exhibit a stronger tendency to enter the ocean via rivers and lakes than high-density plastic debris (Wang et al., 2016b). Polyamide (PA), commonly known as nylon, is a widely used plastic as woven fiber, of which polyamide 6 (PA6) is the most common component. Owing to its excellent mechanical, electrical, and wear resistance properties, PA has also been widely used as an engineering plastic. PA6 MPs are a relatively low-density plastic ($\rho = 1$–1.15 g/cm^3) and widely found in the natural environment around the world, such as rivers (Kataoka et al., 2019), oceans (Andrady, 2011), sediments (Wang et al., 2019), beaches (Lo et al., 2018) and even in living organisms (Cole et al., 2019). Therefore, PA6 MPs have a great possibility to migrate into the natural environment.

As an emerging contaminant, Sulfamethoxazole (SMX) is also widely present in the water environment (Thai et al., 2018). SMX in the water environment not only affects the growth and development of organisms but also induces the production of resistant bacteria or resistance genes (Wang et al., 2016a). It has been shown that MPs can transport the antibiotics into the organism through desorption when the aquatic organisms ingest MPs with surface-loaded contaminants accidentally, thereby adversely affecting the organisms. Unlike the aqueous environment, the complex biological conditions in the organism may

* Corresponding authors.
E-mail addresses: gcyslw@xju.edu.cn (C. Guo), wei.wang@uib.no (W. Wang), awangjd@sina.cn (J. Wang).

https://doi.org/10.1016/j.ecoenv.2023.115400
Received 31 October 2022; Received in revised form 17 August 2023; Accepted 20 August 2023
Available online 29 August 2023

enhance the potential effects of the MPs. Guo et al. (2019b) studied the adsorption behavior of PP、PET、PS、PVC、PE and PA6 MPs for SMX and found that PA6 MPs have a strong sorption capacity for SMX (Guo et al., 2019b). So further studies on the desorption mechanisms of SMX from PA6 MPs are necessary to complement the environmental risk assessment of MPs in gastrointestinal fluids.

Recent research has mainly focused on the potentially toxic effects of MPs on the aquatic ecosystem worldwide. Since MPs can absorb and accumulate pollutants in the surrounding water, a wide range of pollutants are co-present with MPs by being absorbed on their surfaces. Bakir et al. (2014) showed that intestinal surfactants facilitated the desorption rate of pollutants that absorbed on plastics, and the stomachs of organisms were also the site for the desorption of pollutants from MPs (Bakir et al., 2014). Previous studies have reported that simulated biological digestion fluid (simulated gastric fluid and intestinal fluid) can promote the desorption of antibiotic from MPs (Xu et al., 2018; Fan et al., 2021; Fan et al., 2023). Hence, it is necessary to further investigate the adsorption and desorption relationships between PA6 MPs and SMX. The desorption behavior of MPs with surface-loaded contaminants in the gastrointestinal fluids is controlled by integrated factors of plastic properties (crystallinity, pore, volume, and hydrophobicity), gastrointestinal fluid properties (digestive enzyme type, digestive fluid, fraction, and pH) and the contaminants. Unfortunately, the exact mechanism is still unclear, therefore the mechanism of contaminant transfer from PA6 MPs to the gastrointestinal fluids needs to be investigated (Liao and Yang, 2020; Liu et al., 2020b).

Nowadays, the desorption mechanism of SMX from PA6 MPs in the gastrointestinal fluids is still not clear. Therefore, this study intends to provide some detailed information as follows: (1) To investigate the adsorption behavior of PA6 MPs on SMX and further explore the effect of solution pH and salinity on adsorption; (2) The desorption behavior of SMX from PA6 MPs in ultrapure water, seawater, simulated intestinal and gastric fluid conditions have been identified; (3) To explore the effect of desorption under different gastrointestinal conditions (pH, temperature, and salinity); (4) The desorption mechanisms of SMX-loaded PA6 MPs under different conditions were proposed.

2. Experiment

2.1. Materials

Sulfamethoxazole (SMX) (> 98%) was purchased from Aladdin Industrial Corporation (Shanghai, China). SMX was dissolved in acetonitrile for the preparation of a 10 g/L stock solution. Then the stock solution was kept in the dark at 4 °C. PA6 MPs (the mean size of 150 μm) were purchased from Tesulang Chemical Company (Guangdong, China). Pepsin (molecular weight of 35 kDa), bovine serum albumin (BSA, ≥ 98%, molecular weight of 66 kDa), and sodium taurocholate (NaT, ≥ 97%) were all purchased from Aladdin Industrial Corporation (Shanghai, China). All chemicals were used analytical grade or higher purity and solvents were HPLC grade. The properties of selected PA6 MPs were summarized in Table S1.

2.2. Sorption experiments

The sorption experiments were carried out according to batch methods. All experiments were performed in triplicate, The control group used the same method in the same solution of SMX but without MPs.

For SMX sorption kinetic experiments, the initial concentration of SMX was 6.0 mg/L. The final acetonitrile concentration used in experiments was maintained at < 0.1% (v/v) to avoid co-solvent effects during the experiment, and the low acetonitrile content does not affect the overall experimental results. 200 mg PA6 MPs were added into 50 mL brown glass vials with threaded lids containing 40 mL of 6 mg/L SMX, then the vials were shaken in the dark at 25 °C in a thermostatic shaker at 160 rpm. These concentration ranges were determined from a preliminary experiment to guarantee 20%−80% uptake of the sorbates at equilibrium. The adsorption capacity was assessed at time intervals of 0.15, 0.5, 1, 2, 4, 8, 12, 24, and 48 h. The kinetics data showed sorption equilibrium of SMX on PA6 MPs was achieved within 24 h, so 24 h was adopted for subsequent adsorption tests. For the sorption isotherm experiment, the SMX solutions with different concentrations (1, 2, 4, 6, 8, 10, 12 mg/L) were added into the brown glass vials, then the samples were shaken at 160 rpm for 24 h to achieve equilibrium. To examine the effect of pH and salinity, the pH was adjusted in the range of 3–9 with 0.1 mol/L HCl and NaOH; the salinity was adjusted to 5–35‰ using NaCl. The initial concentration of SMX solution was 6 mg/L, and all the samples were shaken at 160 rpm for 24 h. All collected samples were passed through 0.22 μm filters to remove PA6 MPs.

2.3. Desorption in simulated gastric and intestinal conditions

To make the desorption amount easy to detect and to reduce the experimental error, we set the concentration of SMX adsorbed by PA6 MPs to 20 mg/L. The SMX-loaded PA6 MPs were prepared by spiking 20 mg/L SMX solution into 50 mL brown glass vials containing 200 mg PA6 MPs. The mixture was shaken at 160 rpm for 24 h to reach sorption equilibrium according to the adsorption kinetics experiment. After sorption equilibrium, the MPs were collected via vacuum filtration, washed three times with ultrapure water, and then airdried for 48 h. The amount of SMX absorbed onto PA6 MPs was 1.2 mg/g.

The simulated gastric fluid was prepared by adding pepsin in 100 mmol/L of NaCl solution to a final concentration of 3.2 g/L. Simulated intestinal fluid consisted of 5.0 g/L bovine serum albumin (BSA) and 10 mmol/L sodium taurocholate (NaT) in 100 mmol/L NaCl solution (Lee et al., 2019; Mohamed Nor and Koelmans, 2019). The pH of gastric and intestinal fluids was adjusted to 2.0 and 7.0, respectively to mimic the acidic stomach and neutral gut environments. Simulated seawater (550 mmol/L NaCl and pH 7.0) was prepared for comparison (Coffin et al., 2019). For desorption kinetic experiments, 40 mL of gastrointestinal fluid was spiked into a vial containing 200 mg SMX-loaded PA6 MPs, respectively. then incubated in a rotary shaker at 160 rpm for 72 h. The temperature was kept at 18 °C and 37 °C to mimic the gastrointestinal conditions of cold- and warm-blooded marine organisms, respectively (Tanaka et al., 2015). At each sampling point, 1 mL solution was withdrawn and passed through 0.22 μm filters to remove MPs. The residual amounts of SMX on MPs were calculated by mass balance.

Because various types of marine organisms have different gastrointestinal conditions and for the same organism, its gastrointestinal condition may also be different from fasted- to fed-states (Bucking and Wood, 2009), the desorption experiments were performed in various digestion conditions including pH (2.0, 4.5 and 7.0 for gastric fluid, and 4.5, 7.0 and 9.5 for intestinal fluid) and ionic strength (10.0, 100.0 and 200.0 mmol/L of NaCl). Control sorption experiments with no SMX were performed using the reactor system containing PA6 MPs to enhance the experiment's accuracy, and the desorption amount of SMX from PA6 MPs in gastrointestinal fluids was corrected according to control experiments.

2.4. Sorption and solubility experiments

To clarify the desorption mechanisms of SMX from PA6 MPs in gastrointestinal fluids, sorption experiments of PA6 MPs for SMX (1, 2, 4, 6, 8, 10, and 12 mg/L) were conducted under pH 2.0 and 7.0 of background solutions (100.0 mmol/L NaCl) and gastric (3.2 g/L of pepsin) and intestinal fluids (5.0 (g/L)/10 mM of BSA/NaT). The solubility of SMX was tested under various concentrations of pepsin (0.0, 0.4, 0.8, 1.6, 3.2 and 5.0 g/L), BSA (0.0, 0.5, 1.0, 2.5, 5.0 and 7.5 g/L), NaT (0.0, 1.0, 2.0, 5.0, 10.0 and 15.0 mmol/L) and BSA/NaT (0, 0.5/1.0, 1.0/2.0, 2.5/5.0, 5.0/10.0 and 7.5/15.0 (g/L)/mmol/L), and various water pH (2.0, 4.5, 7.0, 9.5 and 11.5). In addition, the sorption

experiments of pepsin (0.5, 1.0, 2.0, 3.0, 4.0, and 5.0 g/L), BSA (0.5, 1.0, 2.0, 3.0, 4.0, and 5.0 g/L) and NaT (1.0, 2.0, 3.0, 4.0, 5.0 and 6.0 g/L) on PA6 MPs were conducted to probe the potential interaction between MPs and gastrointestinal components, respectively.

2.5. PA6 MPs characterization

The zeta potential of PA6 MPs in the solid state was directly measured by an Electrokinetic Analyzer (SurPass 3, Anton Paar, Austria) coupled with the cylindrical cell, avoiding their uneven dispersion in solution. The morphology and microstructure of PA6 MPs were characterized by field-emission scanning electron microscopy (SEM, SU-8010, Hitachi Ltd., Japan). The functional groups of sorbents were observed utilizing a Nexus 670 Fourier transform infrared (FTIR) spectrometer (Nicolet Instrument Corporation, Madison, USA).

2.6. Analytical methods

The amount of SMX absorbed onto PA6 MPs was calculated by Eq. (1):

$$Q_t = \frac{V}{m}(C_o - C_t) \tag{1}$$

where Q_t (mg/g) is the uptake of SMX by MPs, m (g) is the mass of the MPs, V (L) is the volume of SMX solution, C_o (mg/L) and C_t(mg/L) are the initial and final SMX concentrations, respectively.

The pseudo-first-order model (PFOM) and pseudo-second-order model (PSOM) were used to describe the sorption kinetics. The pseudo-first-order model and pseudo-second-order model were applied to explore the adsorption process in detail, which are expressed as follows by Eqs. (2, 3):

$$Pseudo-first\quad order\quad model: Q_t = Q_e\left(1 - e^{-k_1 t}\right) \tag{2}$$

$$Pseudo-second\quad order\quad model: Q_t = \frac{{Q_e}^2 k_2 t}{1 + {Q_e}^2 k_2 t} \tag{3}$$

where k_1 (h^{-1}) and k_2 (g/(mg h)) is the adsorption rate constants for different models; t (h) is adsorption time; The pseudo-first-order model is based on the assumption that the physical diffusion process is the rate-limiting step (Wang and Wang, 2018). In the pseudo-second-order model, the adsorption rate is related to the square of the amount of unoccupied adsorption sites on the adsorbent surface (Zhang et al., 2019), which involves chemical interactions between adsorbents and adsorbates such as electron sharing and electron transfer (Liu, 2018; Zhang et al., 2019).

The adsorption isotherms curves were fitted with the most commonly used isotherm equations (i.e., the Langmuir and Freundlich models) as follows by Eqs. (4, 5):

$$Langmuir\quad model: Q_e = \frac{Q_m K_L c_e}{1 + K_L c_e} \tag{4}$$

$$Freundlich\quad model: Q_e = K_F {c_e}^{1/n} \tag{5}$$

Q_m(mg/g) is the maximum adsorption capacity of per gram of MPs. C_e(mg/L) represents the equilibrium concentration of SMX. K_L (L/g) and K_F (L/g) are the affinity constants of the Langmuir and Freundlich models, respectively. n refers to the surface heterogeneity factor. The Langmuir model demonstrates ideal monolayer adsorption on homogeneous adsorbent surfaces, where each adsorption site exerts the same force on adsorbate molecules (Ma et al., 2019b). The Freundlich model is an empirical formula based on the heterogeneity of adsorbent surfaces (Wang and Wang, 2018).

3. Results and discussion

3.1. Characterization of PA6 MPs

Fig. 1 shows the SEM micrographs of PA6 MPs. The surface of PA6 particles was relatively smooth, several micropores, wrinkles, and cracks can be found on the surface of PA6 MPs. The properties of selected PA6 MPs are listed in Table S1.

The zeta potentials of PA6 MPs in a series of pH conditions are presented in Fig. S1, and the p*K*a values of SMX were 1.83 and 5.57 (Yi et al., 2015). The isoelectric point of SMX is 4.06 according to the calculation through ChemAxon. The different surface charges of PA6 MPs at various pH values may affect the sorption behaviors via electrostatic effects.

3.2. The sorption kinetics and isotherms

The effect of time on the adsorption of SMX by PA6 MPs is shown in Fig. 2. The adsorption process was fast in the beginning, then slowed down, and finally reached dynamic equilibrium. The adsorption process can be divided into 3 main stages: In the first 12 h, the reaction was a fast adsorption process, and the adsorption followed by a slow adsorption stage for the next 12 h. The dynamic adsorption equilibrium was reached a dynamic equilibrium at 24 h with an adsorption capacity of 0.59 mg/g (Fig.2a). This result agrees with previous adsorption studies of antibiotics to MPs in simple water mediums (Xu et al., 2018; Guo et al., 2019b; Liu et al., 2020a). Guo et al. (2019) studied the adsorption of SMX on six types of microplastics (polyamide (PA), polyethylene (PE), polyethylene terephthalate (PET), polystyrene (PS), polyvinyl chloride (PVC) and polypropylene (PP)) and revealed different equilibrium time of antibiotics on microplastics is significantly influenced by the mass transfer limiting steps, which include the external/internal mass transfer, and the adsorption on active sites (Guo et al., 2019a; Kong et al., 2021).

The rate-limiting steps of SMX adsorption on PA6 MPs were investigated by kinetics fitting (Fig.2b). The correlation coefficients (R^2) fitted by the different kinetic models are listed in Table 1. It can be seen that the pseudo-second kinetic model fitted the kinetic data better, which indicates that the adsorption of SMX on PA6 MPs is also probably influenced by the sorption onto surface sites, mass transfer, and intra-particle diffusion was involved in the sorption process. The reason for the above result is mainly the rough surface of PA6 MPs with more cracks and pores which can provide more adsorption sites. This result is consistent with previous research, which has found antibiotics adsorption to MPs fitted the pseudo-second-order model (Liu et al., 2020a; Yu et al., 2020).

The adsorption isotherms can reveal the equilibrium state of the adsorbate in solution and adsorbent, and further clarify the occurrence of the adsorption mechanism. Fig. 3a shows the adsorption isotherm data of SMX on PA6 MPs. To investigate the mechanism of SMX adsorption on PA6 MPs, Freundlich, and Langmuir isotherms were used for the isotherm data, as shown in Table 1 and Fig.3b. In general, the Freundlich model fits better ($R^2 \geq 0.997$) than Langmuir ($R^2 \geq 0.985$), indicating that the adsorption of SMX on PA6 MPs is the heterogeneous multi-layer sorption process. PA6 MPs have amide groups in which both O and N can easily form hydrogen bonds with the H atoms of the two amine parts of the SMX structure. Therefore, the formation of hydrogen bonding may be the possible mechanism for the adsorption of SMX by PA6 MPs. This result can also be drawn from FTIR images in Fig. S2. The Freundlich constant K_F value for PA6 was 0.0919 L/g, indicating that the adsorption was favorited and PA6 MPs had a high affinity for SMX. Similar trends were reported that the Freundlich model fitted the sorption data of SMX on MPs well (Xu et al., 2018; Guo et al., 2019b).

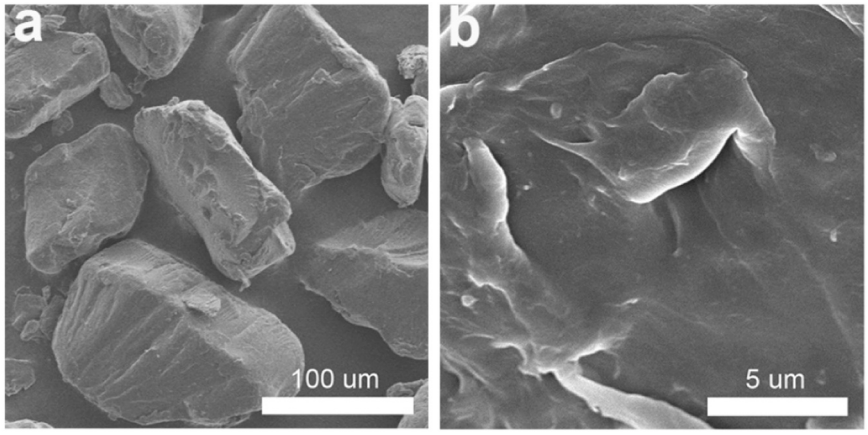

Fig. 1. SEM micrographs of PA6 MPs.

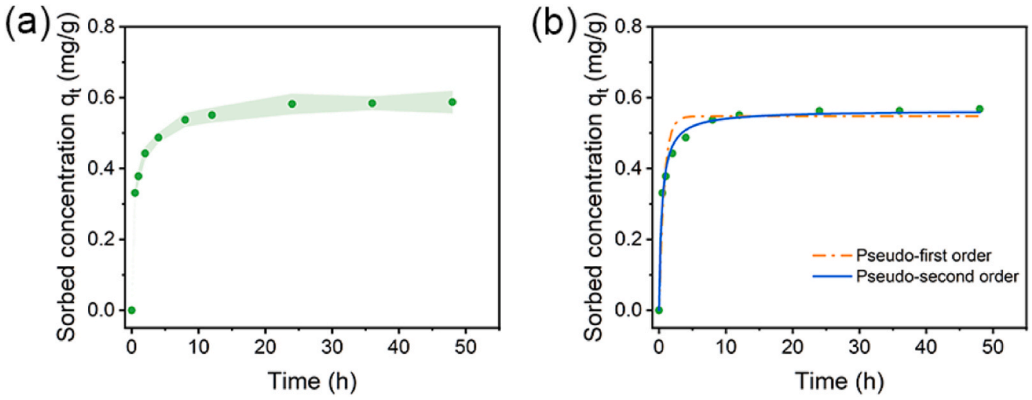

Fig. 2. (a) Adsorption of PA6 MPs for SMX; (b) The fitting curves of adsorption kinetic models.

Table 1
Parameters of the kinetics and isotherm models for sorption experimental data of SMX on PA6 MPs.

Model	Type	Parameter	PA6 MPs
Kinetics	Pseudo-first order	q_1 (mg/g)	0.5475 ± 0.0184
		K_1 (g/(mg h))	1.3259 ± 0.2341
		R^2	0.934
	Pseudo-second order	q_e (mg/g)	0.5641 ± 0.0078
		K_2 (g/(mg h))	4.0617 ± 0.4362
		R^2	0.991
Isotherm	Freundlich	K_F (L/g)	0.0919 ± 0.0076
		N	1.0723 ± 0.0429
		R^2	0.997
	Langmuir	q_m (mg/g)	7.0992 ± 3.1733
		K_L (L/g)	0.0125 ± 0.0062
		R^2	0.985

3.3. The influence of salinity and pH

To simulate the change of salinity from the river to the ocean, the salinity gradient for the corresponding experiments was set from 5‰ to 35‰ in NaCl solution to observe the effect of the ionic strength underwater conditions. Fig. 4a results suggest that the change of salinity can significantly affect the adsorption of SMX by PA6 MPs, While the sorption capacities of SMX on PA6 MPs decreased slightly with higher salinity. Previous researches have examined the effect of salinity on the sorption behaviors of microplastics. Li et al. (2018) demonstrated that the sorption of antibiotics on microplastics in seawater was lower than the sorption capacities in freshwater (Li et al., 2018). Llorca et al. (2018) reported that the uptakes of PFAS by microplastics decreased in seawater. The concentrations of Na^+ increased with increasing salinity. Since the surface of microplastics is negatively charged, the positively charged Na^+ is easier to be sorbed on microplastics by electrostatic attraction reactions (Llorca et al., 2018). The acidic groups of microplastics may be substituted by H^+ in this process, which could influence the formation of hydrogen bonding (Aristilde et al., 2010). Thus, the sorption capacities of SMX on microplastics decreased. It indicated that the electrostatics interactions may play an important part, and the formation of hydrogen bonding is presumed to be the main mechanism in this process.

The pH can not only affect the surface charge of the MPs but also determine the molecular morphology of SMX in solution, which can potentially alter the interaction between the MPs and SMX. The effect of the pH change in the solution is shown in Fig. 4b. The adsorption capacity under alkaline conditions was significantly lower than the acidic and neutral conditions. SMX are ionizable compounds, but the ionization constant (p*K*a) of SMX usually differed significantly because of the specific functional groups. Thus, in a specific pH condition, SMX will exhibit different speciation of the cation (pH < p*K*a1), zwitterion (p*K*a1 < pH < p*K*a2), and anion (pH > p*K*a2). The speciation of ionic chemicals can influence their sorption extent on MPs. The p*K*a1 and p*K*a2 values of SMX are 1.83 and 5.57, respectively (Yi et al., 2015). When the pH in water is less than 1.83, the positively charged SMX^+ is the main ion species and SMX mainly exists in neutral forms within the pH range of 1.83 – 5.57 and transforms to anionic species within pH range of 5.57 – 9.00. Microplastics polymers are always negatively charged in alkaline solutions and the surface of microplastics is inclined to be protonated with decreasing pH values. Since the electro negativity of the surface of PA6 MPs increases with the increase of pH values, the

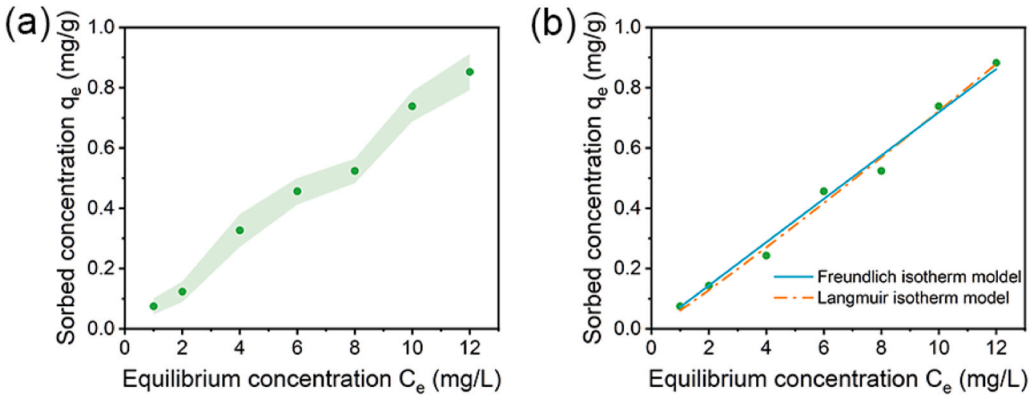

Fig. 3. (a) The effect of initial concentration of SMX on PA6 MPs; (b) the fitting graphs of adsorption isotherms models.

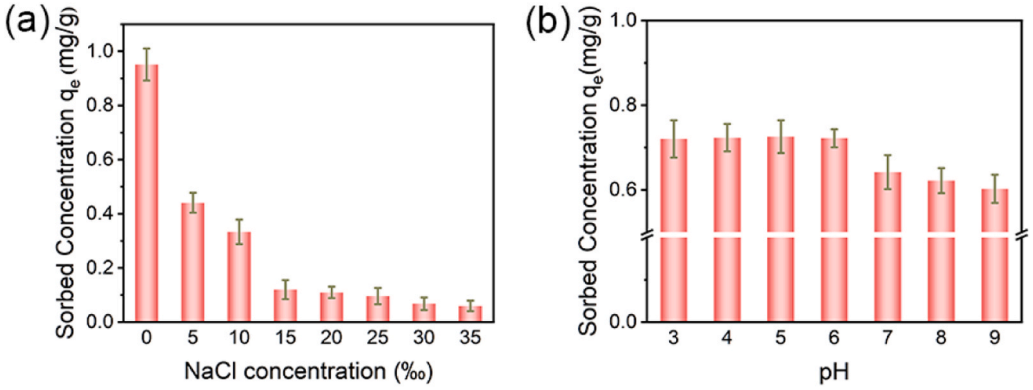

Fig. 4. The influences of (a) NaCl concentration and (b) pH on adsorption of SMX by PA6 MPs.

electrostatic repulsion can decrease the sorption capacity of SMX on PA6 MPs in an alkaline environment. Laboratory evidence showed that the increase of pH decreased the sorption of humic acid (HA) on PS, PVC (Zhang et al., 2022), triclosan on PVC (Ma et al., 2019a), and tylosin on PS and PVC (Guo et al., 2018), which were in agreement with our results. This result suggests that electrostatic interactions also affect the adsorption behavior of MPs in the adsorption process.

3.4. Desorption mechanisms in gastric and intestinal conditions

3.4.1. Desorption kinetics of SMX from PA6 MPs

The desorption kinetics of different matrices were investigated at an average adsorption concentration (1.2 mg/g) of SMX by PA6 MPs. Fig. 5a represents the desorption kinetic curves of PA6 MPs under four simulated conditions, which can be found that the highest desorption capacity of SMX-loaded PA6 MPs was 0.7 mg/g with 59.9% desorption rate in simulated seawater due to the higher ionic strength. Moreover, the high desorption capacity in the simulated intestinal fluid was 0.7 mg/g with a 58.3% desorption rate, which is probably because of the neutral pH, higher ionic strength, and the solubilization of SMX by the intestinal fluid components BSA and NaT. In the simulated gastric fluid, the high desorption capacity was 0.5 mg/g with a 45.4% desorption rate due to the acidic pH, the high ionic strength, and the solubilization of SMX by the gastric fluid component pepsin. The lowest desorption capacity was 0.4 mg/g with a 36.4% desorption rate in ultrapure water. Previous research has found an increased desorption of fluoxetine from

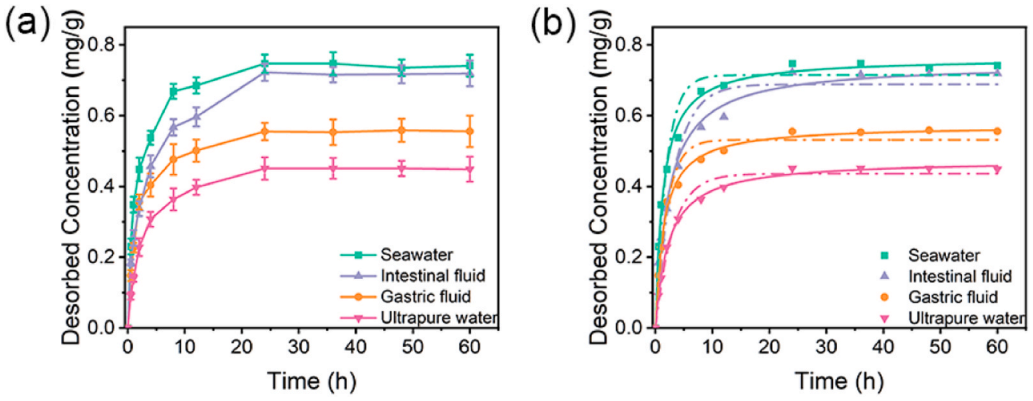

Fig. 5. (a) Desorption time of SMX; (b) Desorption kinetics of SMX on PA6 MPs in various desorption conditions and the fitting curves of adsorption kinetic models. The solid line and dash line represent the desorption kinetics fitted by the pseudo-first-order model and the pseudo-second-order model, respectively.

polyethylene MPs in gastric fluids compared to intestinal fluids and river water (McDougall et al., 2022). Therefore, once ingested by organisms, the SMX-loaded PA6 MPs would pose a high risk to the organisms due to the potential dual bio-toxic effects.

The desorption rate of SMX-loaded PA6 MPs under all four desorption conditions was fast in the first 20 h, and then the desorption rate decreased significantly. The fast desorption phase can be completed within 20 h, whereas the slow desorption phase will last from several months to several years. Usually, The rapid desorption phase is more important for assessing the desorption behavior of SMX in the simulated gastrointestinal tract because the actual digestion time of marine organisms is limited. The desorption data for SMX-loaded PA6 MPs fitted with the pseudo-first-order and the pseudo-second-order kinetic models is shown in Fig. 5b and Table 2. The pseudo-second kinetic model fitted the desorption kinetic data well with R^2 (0.977–0.997), which is also inconsistent with the adsorption kinetic data.

Fig. S3 shows that when the temperature was increased to 37 °C, the desorption rate was faster in the first 10 h and slower thereafter. Since the rapid desorption phase can be completed within 10 h with temperature changing from 18° to 37°C, therefore increasing the temperature could accelerate desorption. The desorption capacity in gastric fluid increased to 0.6 mg/g with a 48.6% desorption rate, and the desorption capacity in intestinal fluid increased to 0.7 mg/g with a 64.0% desorption rate, respectively. The rate constant of desorption was K_2 (simulated intestinal fluid 37 °C) = 1.0586 > K_2 (simulated intestinal fluid 18 °C) = 0.6304; K_2 (simulated gastric fluid 37 °C) = 1.2317 > K_2 (simulated gastric fluid 18 °C) = 0.5929. This result further indicates that high temperature enhances the desorption of SMX in gastric fluid, which means increasing ambient temperature, cold-blooded organisms have higher utilization of SMX-loaded PA6 MPs. Once organisms ingest SMX-loaded PA6 MPs accidentally, there is a high probability of SMX transfer from the microplastic surface to the gastrointestinal fluids.

3.4.2. Desorption of SMX from PA6 MPs in various gastric and intestinal conditions

The desorption behavior of SMX in PA6 MPs under different gastrointestinal conditions was further investigated by examining different digestion ratios. From the effect of pH on desorption shown in Fig. 6a, it can be found that when gastric pH increased from 2.0 to 7.0, the capacity of desorption increased by 1.2–1.3 times, and the desorption capacity in intestinal fluid increased 2.2–2.3 times when intestinal pH increased from 4.5 to 9.5. The significantly promoted desorption of SMX in PA6 MPs may be due to the different solubility of SMX at different pH conditions. SMX has a higher solubility at high pH conditions (Fig. S4). The difference in SMX solubility affects their partitioning between MPs and the aqueous phase, which reduces the electrostatic interaction between the surface charge of the MPs and the antibiotic, subsequently altering the desorption of SMX from the MPs.

Fig. 6b shows that salinity has less effect on the desorption of SMX from PA6 MPs, and the increase in salinity inhibits the desorption in gastric fluid. On the one hand, high salinity induced the salting-out effect of organic compounds, hence enhancing the partition of chemicals on MPs (Wu et al., 2016), which might explain the reduced desorption in the gastric and intestinal fluids. Moreover, high salinity results in the structural change and salting-out effect of pepsin (Kristiansen et al., 2008; Mahapatra and Roy, 2019), which potentially affects the interactions of pepsin with antibiotics and MPs, and then decrease the desorption of SMX. On the other hand, the increased salinity can neutralize the surface charges on MPs via the compression of the electric double layer. NaCl can inhibit mass transfer from the aqueous to the solid phase by increasing the viscosity and density of the solution, thus enhancing the desorption of SMX on PA6 MPs, which is also consistent with the previous results of salinity on adsorption experiments where high ionic strength can inhibit adsorption and thus increase desorption.

3.4.3. Solubilization of SMX by the gastric and intestinal components

The solubility of the SMX was measured under various concentrations of pepsin and BSA/NaT, respectively (Fig. 7). For SMX, its solubility gradually decreased from 0.3 to 0.27 g/L when the concentrations of pepsin increased from 0.5 to 5 g/L (Fig. 7b). However, the solubility of SMX was slightly increased compared to the solubility of SMX in ultrapure water (pH = 7). Moreover, the solubility of SMX was increased from 0.18 to 0.58 g/L in the concentration ranges of BSA/NaT from 0 to 5/10 (g/L)/mM, which indicates that the solubilization effect of pepsin and BSA/NaT to the SMX (Fig. 7a). The increased solubility cannot only enhances the hydrophilic interaction between SMX and MPs but also increases the partition of SMX in aqueous phase (Wang et al., 2011). From Fig. 7a, BSA/NaT exhibited the higher solubilizing ability to SMX than pepsin, thus supporting the higher desorption amount in intestinal fluid.

Which components (BSA or NaT) play a major role in enhancing the solubilization of SMX was further investigated in the intestinal fluid. As shown in Fig. (7c, d), both BSA and NaT enhanced the dissolution of SMX by maximum factors of 6 compared to that in ultrapure water, indicating the similar roles of BSA and NaT in promoting the desorption of SMX in intestinal fluid. For example, the solubility of SMX was 0.59 g/L in 5 g/L of BSA solution (used in the desorption tests), which was 1.7 times higher than that in 10 mM of NaT solution. This indicates that BSA plays a more important role in driving the desorption of SMX than NaT in intestinal fluid.

3.4.4. Adsorption of SMX on PA6 MPs in the gastric and intestinal conditions

To date, there are few studies on the desorption mechanism of

Table 2
Parameters of the kinetics data for desorption of SMX from PA6 MPs in the simulated seawater, ultrapure water, gastric and intestinal fluids.

Type		Parameter	Desorption matrix					
			Ultrapure water at 25 °C	Sea water at 25 °C	Gastric fluid at 18 °C	Gastric fluid at 37 °C	Intestinal fluid at 18 °C	Intestinal fluid at 37 °C
Kinetics	Pseudo-first order	q_1 (mg/g)	0.4310 ± 0.0123	0.7094 ± 0.0191	0.6885 ± 0.0025	0.5314 ± 0.0143	0.6690 ± 0.0301	0.7519 ± 0.0278
		K_1 (g/(mg h))	0.3364 ± 0.0374	0.5531 ± 0.0751	0.3141 ± 0.04816	0.4975 ± 0.0618	0.3530 ± 0.0619	0.5538 ± 0.0958
		R^2	0.966	0.932	0.934	0.934	0.913	0.930
	Pseudo-second order	q_2 (mg/g)	0.4757 ± 0.0050	0.7622 ± 0.0090	0.7486 ± 0.0157	0.5714 ± 0.0068	0.7397 ± 0.0206	0.8000 ± 0.0193
		K_2 (g/(mg h))	0.9360 ± 0.0501	1.0253 ± 0.0773	0.5929 ± 0.0694	1.2317 ± 0.0909	0.6304 ± 0.0887	1.0586 ± 0.1604
		R^2	0.997	0.991	0.988	0.991	0.977	0.977

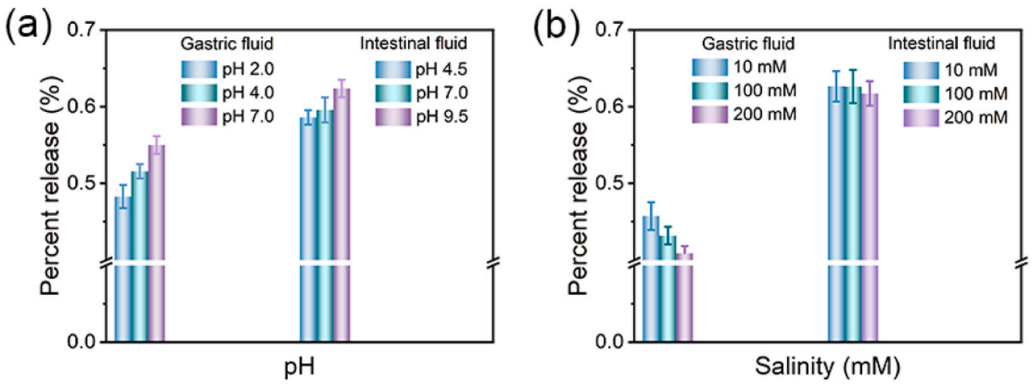

Fig. 6. Desorption of SMX from PA6 MPs under different (a) pH; (b) salinity in gastric and intestinal fluids.

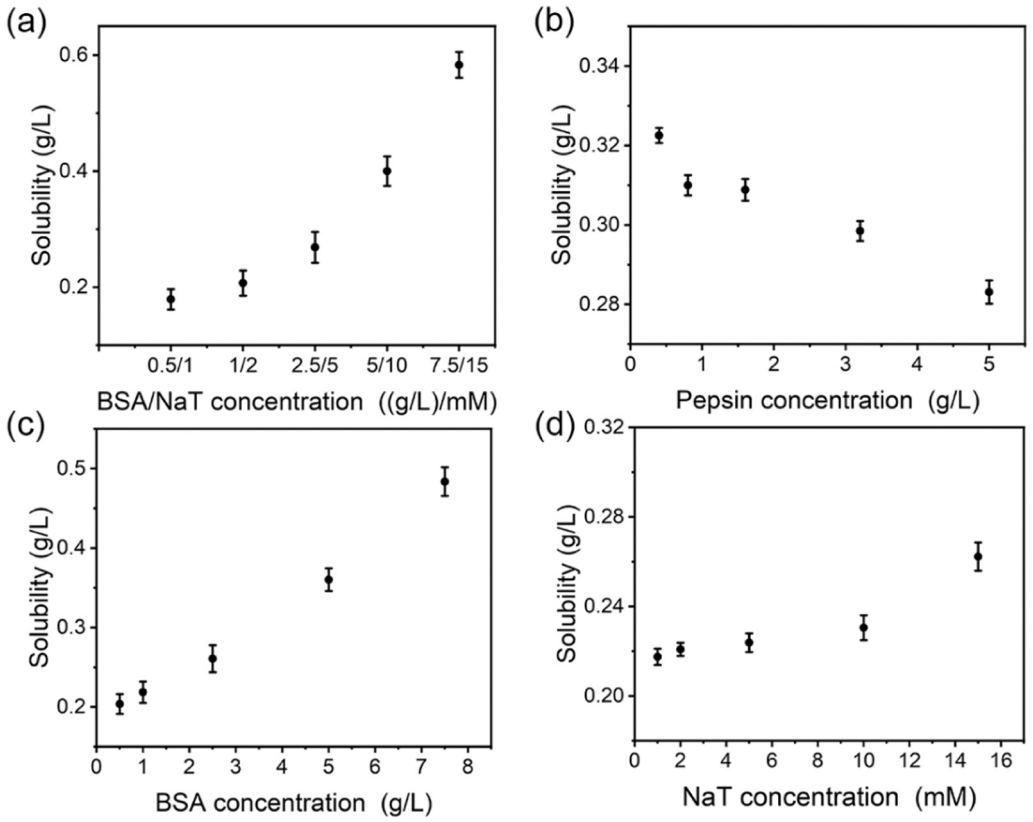

Fig. 7. Solubility of SMX in various concentrations of (a) BSA/NaT; (b) Pepsin; (c) BSA and (d) NaT solutions.

contaminants from MPs into the gastrointestinal fluids. SMX was absorbed on PA6 MPs in gastric fluid, background solution I, intestinal fluid, and background solution II. According to Table 3 and Fig. S5, it can be found that the adsorption process onto PA6 MPs was both well fitted by Langmuir and Freundlich models. By comparing R^2 values, it can be observed that the R^2 values calculated by the Freundlich model (0.969–0.999) were higher than those calculated by the Langmuir model (0.963–0.999). Such results indicated that the Freundlich model is more suitable for simulating SMX adsorption than the Langmuir model. Freundlich isotherm adsorption is non-uniform adsorption that is not limited to a single molecular layer, which suggests that the adsorption of SMX on PA6 MPs in four conditions is non-uniform adsorption of multilayers. The reason for the above result may be due to the non-uniform distribution of adsorption sites on the surface of the PA6 MPs. K_F and N are related to the adsorption amount and intensity.

Table 3 suggests that the K_F of gastric and intestinal fluids changes little compared with their background solutions, K_F (gastric fluid) = 0.184 L/g, K_F (background solution i) = 0.182 L/g, K_F (intestinal fluid) = 0.020 L/g and K_F (background solution ii) = 0.021 L/g, which indicates that the gastrointestinal components have a certain effect on the adsorption of PA6 MPs. This result is also consistent with the adsorption experimental results of SMX on PA6 MPs in the gastrointestinal components. It was also found that the adsorption amount of SMX on PA6 MPs increased under the gastric and background solution conditions, while decreasing under the intestinal and background solution conditions. In the previous adsorption isotherm experiment, K_F = 0.092 L/g, which is significantly lower than gastric conditions but higher than intestinal conditions, further indicates that the adsorption of SMX on PA6 MPs in the gastrointestinal fluids is caused by a variety of factors such as solubilization of SMX by the gastrointestinal components, ionic strength and pH of the solution, but not related to the PA6 MPs themselves.

Table 3
Adsorption isotherm parameter of SMX on PA6 MPs in gastrointestinal fluids relative to those in background solutions.

Kinetics	Type	Parameter	Sorption matrix			
			Background[I]	Background[II]	Gastric fluid	Intestinal fluid
Isotherm	Freundlich	K_F (L/g)	0.182 ± 0.001	0.020 ± 0.001	0.184 ± 0.002	0.021 ± 0.001
		N	1.0057 ± 0.0001	1.3442 ± 0.0089	1.0089 ± 0.0001	1.3541 ± 0.0093
		R^2	0.999	0.970	0.999	0.969
	Langmuir	q_{max} (mg/g)	145.1392 ± 34.4987	0.4457 ± 0.0683	281.8240 ± 179.6480	0.3159 ± 0.0512
		K_L (L/g)	0.0013 ± 0.0003	0.0338 ± 0.0006	0.0006 ± 0.0004	0.0549 ± 0.0251
		R^2	0.999	0.992	0.999	0.963

3.4.5. Sorption of gastric and intestinal components on PA6 MPs

A new sorption-desorption equilibrium was established when the SMX-loaded MPs were introduced into an antibiotic-free solution, and during this period, the gastrointestinal components might occupy the sorption sites on MPs and drive the desorption of SMX-loaded MPs. The competitive sorption between SMX and pepsin or BSA/NaT on PA6 MPs was investigated. Unfortunately, the pepsin, BSA, and NaT were not absorbed on the PA6 MPs after 60 h according to the adsorption contact time curve, and this result is also consistent with the adsorption results of PA6 MPs on SMX in gastrointestinal conditions. In terms of desorption mechanisms, the ability to desorb contaminants from the surface of MPs depends on the strength of the interfacial bond between the contaminants and the MPs. In the gastrointestinal environment, the interfacial binding of MPs to contaminants changes, resulting in the detachment of contaminants from the surface of MPs, and the strength of the interfacial binding is influenced by a combination of the physicochemical properties of MPs (e.g., functional groups, specific surface area, micropore volume, and crystallinity) and the nature of the loaded contaminants themselves. The desorption of contaminants from MPs in the gastrointestinal tract is regulated by a combination of factors and interactions, and the degree of desorption changes dynamically at different stages of the gastrointestinal tract, depending on the solution environment (Liao and Yang, 2020; Liu et al., 2020b).

4. Conclusion

In this study, the adsorption-desorption behavior of PA6 MPs on SMX was investigated. The results indicate that the adsorption of SMX by PA6 MPs reached equilibrium after 24 h, the adsorption kinetics was in accordance with the pseudo-second kinetic model, and the adsorption isotherms fitted with the Freundlich model well. The adsorption capacity varied with environmental conditions (e.g., ionic strength and pH), and the increased desorption capacity in simulated seawater was mainly dependent on the ionic strength of the seawater. In gastrointestinal fluids, the solubilization of gastrointestinal components, ionic strength, and pH of the solution were responsible for the increase of desorption. Once SMX-loaded MPs are ingested by organisms accidentally, they will produce potential dual bio-toxic effects and pose a high risk to organisms. This study reveals important information about the contaminant-loaded environmental MPs to the gastrointestinal fluids of marine organisms. Insights into the desorption mechanism of contaminants from PA6 MPs to the organisms is important for assessing the ecological risk in the environment. Based on these results, future studies should focus on the joint toxicity mechanism of MPs and SMX in marine organisms.

CRediT authorship contribution statement

Kefu Wang: Conceptualization, Methodology, Validation, Formal analysis, Investigation, Data curation, Writing – original draft, Writing – review & editing, Visualization. **Kangkang Wang:** Validation, Formal analysis, Writing – review & editing, Visualization. **Yaoyao Chen:** Software, Data analysis, Writing – review & editing. **Siqi Liang:** Investigation, Formal analysis. **Changyan Guo:** Methodology, Resources, Investigation, Formal analysis, Writing – review & editing, Visualization. **Yi Zhang:** Writing – review & editing, Visualization. **Wei Wang:** Project administration, Funding acquisition, Writing – review & editing. **Jide Wang:** Writing – review & editing Supervision, Project administration, Funding acquisition.

Declaration of Competing Interest

The authors declare that they have no known competing financial interests or personal relationships that could have appeared to influence the work reported in this paper.

Data availability

Data will be made available on request.

Acknowledgements

This research was financially supported by the National Natural Science foundation of China (No. 32061133005) and the Research Council of Norway (RCN, project 320456).

Appendix A. Supporting information

Supplementary data associated with this article can be found in the online version at doi:10.1016/j.ecoenv.2023.115400.

References

Andrady, A.L., 2011. Microplastics in the marine environment. Mar. Pollut. Bull. 62, 1596–1605.
Aristilde, L., Marichal, C., Miéhé-Brendlé, J., Lanson, B., Charlet, L., 2010. Interactions of oxytetracycline with a smectite Clay: a spectroscopic study with molecular simulations. Environ. Sci. Technol. 44, 7839–7845.
Bakir, A., Rowland, S.J., Thompson, R.C., 2014. Enhanced desorption of persistent organic pollutants from microplastics under simulated physiological conditions. Environ. Pollut. 185, 16–23.
Bradney, L., Wijesekara, H., Palansooriya, K.N., Obadamudalige, N., Bolan, N.S., Ok, Y. S., Rinklebe, J., Kim, K.-H., Kirkham, M.B., 2019. Particulate plastics as a vector for toxic trace-element uptake by aquatic and terrestrial organisms and human health risk. Environ. Int. 131, 104937.

Bucking, C., Wood, C.M., 2009. The effect of postprandial changes in pH along the gastrointestinal tract on the distribution of ions between the solid and fluid phases of chyme in rainbow trout. Aquac. Nutr. 15, 282–296.
Coffin, S., Lee, I., Gan, J., Schlenk, D., 2019. Simulated digestion of polystyrene foam enhances desorption of diethylhexyl phthalate (DEHP) and In vitro estrogenic activity in a size-dependent manner. Environ. Pollut. 246, 452–462.
Cole, M., Lindeque, P., Halsband, C., Galloway, T.S., 2011. Microplastics as contaminants in the marine environment: a review. Mar. Pollut. Bull. 62, 2588–2597.
Cole, M., Coppock, R., Lindeque, P.K., Altin, D., Reed, S., Pond, D.W., Sørensen, L., Galloway, T.S., Booth, A.M., 2019. Effects of nylon microplastic on feeding, lipid accumulation, and moulting in a coldwater copepod. Environ. Sci. Technol. 53, 7075–7082.
Fan, X., Zou, Y., Geng, N., Liu, J., Hou, J., Li, D., Yang, C., Li, Y., 2021. Investigation on the adsorption and desorption behaviors of antibiotics by degradable MPs with or without UV ageing process. J. Hazard. Mater. 401, 123363.
Fan, X., Qian, S., Bao, Y., Sha, H., Liu, Y., Cao, B., 2023. Desorption behavior of antibiotics by microplastics (tire wear particles) in simulated gastrointestinal fluids. Environ. Pollut. 323, 121252.
Guo, X., Pang, J., Chen, S., Jia, H., 2018. Sorption properties of tylosin on four different microplastics. Chemosphere 209, 240–245.
Guo, X., Chen, C., Wang, J., 2019a. Sorption of sulfamethoxazole onto six types of microplastics. Chemosphere 228, 300–308.
Guo, X., Chen, C., Wang, J.J.C., 2019b. Sorption of sulfamethoxazole onto six types of microplastics. Chemosphere 228, 300–308.
Kataoka, T., Nihei, Y., Kudou, K., Hinata, H., 2019. Assessment of the sources and inflow processes of microplastics in the river environments of Japan. Environ. Pollut. 244, 958–965.
Kong, F., Xu, X., Xue, Y., Gao, Y., Zhang, L., Wang, L., Jiang, S., Zhang, Q., 2021. Investigation of the adsorption of sulfamethoxazole by degradable microplastics artificially aged by chemical oxidation. Arch. Environ. Contam. Toxicol. 81, 155–165.
Kristiansen, E., Pedersen, S.A., Zachariassen, K.E., 2008. Salt-induced enhancement of antifreeze protein activity: a salting-out effect. Cryobiology 57, 122–129.
Lee, H., Lee, H.-J., Kwon, J.-H., 2019. Estimating microplastic-bound intake of hydrophobic organic chemicals by fish using measured desorption rates to artificial gut fluid. Sci. Total Environ. 651, 162–170.
Li, J., Zhang, K., Zhang, H., 2018. Adsorption of antibiotics on microplastics. Environ. Pollut. 237, 460–467.
Liao, Y.-l, Yang, J.-y, 2020. Microplastic serves as a potential vector for Cr in an in-vitro human digestive model. Sci. Total Environ. 703, 134805.
Liu, P., Wu, X., Liu, H., Wang, H., Gao, S., 2020a. Desorption of pharmaceuticals from pristine and aged polystyrene microplastics under simulated gastrointestinal conditions. J. Hazard. Mater. 392, 122346.
Liu, X., Gharasoo, M., Shi, Y., Sigmund, G., Hüffer, T., Duan, L., Wang, Y., Ji, R., Hofmann, T., Chen, W., 2020b. Key physicochemical properties dictating gastrointestinal bioaccessibility of microplastics-associated organic xenobiotics: insights from a deep learning approach. Environ. Sci. Technol. 54, 12051–12062.
Liu, Y., 2018. Estimating the elasticity of supply of housing space rather than units. Reg. Sci. Urban Econ. 68, 1–10.
Llorca, M., Schirinzi, G., Martínez, M., Barceló, D., Farré, M., 2018. Adsorption of perfluoroalkyl substances on microplastics under environmental conditions. Environ. Pollut. 235, 680–691.
Lo, H.-S., Xu, X., Wong, C.-Y., Cheung, S.-G., 2018. Comparisons of microplastic pollution between mudflats and sandy beaches in Hong Kong. Environ. Pollut. 236, 208–217.
Ma, J., Zhao, J., Zhu, Z., Li, L., Yu, F., 2019a. Effect of microplastic size on the adsorption behavior and mechanism of triclosan on polyvinyl chloride. Environ. Pollut. 254, 113104.
Ma, J., Zhao, J., Zhu, Z., Li, L., Yu, F., 2019b. Effect of microplastic size on the adsorption behavior and mechanism of triclosan on polyvinyl chloride. Environ. Pollut. 254, 113104.
Mahapatra, K., Roy, S., 2019. An insight into the folding and stability of Arabidopsis thaliana SOG1 transcription factor under salinity stress in vitro. Biochem. Biophys. Res. Commun. 515, 531–537.
McDougall, L., Thomson, L., Brand, S., Wagstaff, A., Lawton, L.A., Petrie, B., 2022. Adsorption of a diverse range of pharmaceuticals to polyethylene microplastics in wastewater and their desorption in environmental matrices. Sci. Total Environ. 808, 152071.
Mohamed Nor, N.H., Koelmans, A.A., 2019. Transfer of PCBs from microplastics under simulated gut fluid conditions is biphasic and reversible. Environ. Sci. Technol. 53, 1874–1883.
Stollberg, N., Kröger, S.D., Reininghaus, M., Forberger, J., Witt, G., Brenner, M., 2021. Uptake and absorption of fluoranthene from spiked microplastics into the digestive gland tissues of blue mussels, Mytilus edulis L. Chemosphere 279, 130480.
Tanaka, K., Takada, H., Yamashita, R., Mizukawa, K., Fukuwaka, M.-a, Watanuki, Y., 2015. Facilitated leaching of additive-derived PBDEs from plastic by seabirds' stomach oil and accumulation in tissues. Environ. Sci. Technol. 49, 11799–11807.
Thai, P.K., Ky, L.X., Binh, V.N., Nhung, P.H., Nhan, P.T., Hieu, N.Q., Dang, N.T.T., Tam, N.K.B., Anh, N.T.K., 2018. Occurrence of antibiotic residues and antibiotic-resistant bacteria in effluents of pharmaceutical manufacturers and other sources around Hanoi, Vietnam. Sci. Total Environ. 645, 393–400.
Thompson, R.C., Olsen, Y., Mitchell, R.P., Davis, A., Rowland, S.J., John, A.W., McGonigle, D., Russell, A.E., 2004. Lost at sea: where is all the plastic. Science 304, 838.
Wang, H., Wang, N., Wang, B., Zhao, Q., Fang, H., Fu, C., Tang, C., Jiang, F., Zhou, Y., Chen, Y., Jiang, Q., 2016a. Antibiotics in drinking water in shanghai and their contribution to antibiotic exposure of school children. Environ. Sci. Technol. 50, 2692–2699.
Wang, J., Tan, Z., Peng, J., Qiu, Q., Li, M., 2016b. The behaviors of microplastics in the marine environment. Mar. Environ. Res. 113, 7–17.
Wang, J., Wang, M., Ru, S., Liu, X., 2019. High levels of microplastic pollution in the sediments and benthic organisms of the South Yellow Sea, China. Sci. Total Environ. 651, 1661–1669.
Wang, W., Wang, J., 2018. Comparative evaluation of sorption kinetics and isotherms of pyrene onto microplastics. Chemosphere 193, 567–573.
Wang, Z., Zhao, J., Song, L., Mashayekhi, H., Chefetz, B., Xing, B., 2011. Adsorption and desorption of phenanthrene on carbon nanotubes in simulated gastrointestinal fluids. Environ. Sci. Technol. 45, 6018–6024.
Wu, C., Zhang, K., Huang, X., Liu, J., 2016. Sorption of pharmaceuticals and personal care products to polyethylene debris. Environ. Sci. Pollut. Res. 23, 8819–8826.
Xu, B., Liu, F., Brookes, P.C., Xu, J., 2018. The sorption kinetics and isotherms of sulfamethoxazole with polyethylene microplastics. Mar. Pollut. Bull. 131, 191–196.
Yi, X., Bayen, S., Kelly, B.C., Li, X., Zhou, Z., 2015. Improved detection of multiple environmental antibiotics through an optimized sample extraction strategy in liquid chromatography-mass spectrometry analysis. Anal. Bioanal. Chem. 407, 9071–9083.
Yu, F., Yang, C., Huang, G., Zhou, T., Zhao, Y., Ma, J., 2020. Interfacial interaction between diverse microplastics and tetracycline by adsorption in an aqueous solution. Sci. Total Environ. 721, 137729.
Zhang, J., Zhan, S., Zhong, L.B., Wang, X., Qiu, Z., Zheng, Y.M., 2022. Adsorption of typical natural organic matter on microplastics in aqueous solution: kinetics, isotherm, influence factors and mechanism. J. Hazard Mater. 443, 130130.
Zhang, X., Zheng, M., Yin, X., Wang, L., Lou, Y., Qu, L., Liu, X., Zhu, H., Qiu, Y., 2019. Sorption of 3,6-dibromocarbazole and 1,3,6,8-tetrabromocarbazole by microplastics. Mar. Pollut. Bull. 138, 458–463.